Available online at www.joac.info

ISSN: 2278-1862

Journal of Applicable Chemistry

2014, 3 (1): 310-323

(International Peer Reviewed Journal)

Carica papaya seeds – Green Inhibitor for Corrosion Control of Aluminium in Acid Medium

Pushpanjali M, Suma A Rao and Padmalatha*

* Department of Chemistry, Manipal Institute of Technology, Manipal University, Karnataka, 576104, **INDIA**

Email: padmalatha.rao@manipal.edu.

Accepted on 28th December 2013

ABSTRACT

The inhibitive effect of Carica papaya seed extract (CPSE) on the corrosion behavior of aluminium in H_2SO_4 at pH 2.6 was investigated by using Tafel polarization and electrochemical impedance spectroscopy (EIS) techniques in the temperature range 30°C to 50°C. The concentration of inhibitors used was in the range of 50-400ppm. The surface morphology was studied using scanning electron microscopy (SEM). Inhibition efficiency was found to increase with increase in inhibitor concentration and decrease with increase in temperature. CPSE acted as a mixed type of inhibitor. The inhibitor adsorbed physically on the surface of the metal and followed Langmuir adsorption isotherm. Maximum Inhibition efficiency obtained was 96.7%. The kinetic and thermodynamic parameters were calculated and discussed in detail. The results obtained by both the methods were in good agreement with one another.

Keywords: Corrosion inhibition, Electrochemical techniques, Carica papaya, Adsorption isotherm.

INTRODUCTION

Aluminium has a remarkable industrial importance due to its light weight and low cost. It is used in electronics, for production of wires, sheets, tubes and also to form alloys. Aluminium and aluminium alloys are resistant to corrosion due to the formation of stable oxide layer on the surface. However, when they are exposed to severe acidic and alkaline environment, the protective layer breaks down, and they become prone for corrosion. Aluminium and its alloys are exposed to the action of acid in industrial processes where acid plays an important role such as oil well acidizing, acid pickling, acid cleaning and descaling. This can lead to substantial metal loss due to corrosion [1]. Acid solutions mainly hydrochloric and sulphuric acids are routinely used for the removal of undesirable scale and rust in several industrial processes.

The use of inhibitors is one of the most practical options to protect metal from corrosion. Generally, organic and inorganic compounds are usually added to H_2SO_4 as corrosion inhibitors. The organic inhibitors containing nitrogen, sulphur, and oxygen as heteroatoms, forms coordinate bond with the metal and forms a barrier between metal and corrosive medium. However, synthesis of these compounds may involve the use of harmful chemicals, which are relatively costly. Harmful effects of these chemicals received global attention and there is growing demand for cheaper, non-toxic and environmentally benign

corrosion inhibitors. [2] Now a days plant product are emerged as efficient alternates [3].These natural products serve as a rich source of heterocyclic compounds which are proven to be excellent corrosion inhibitors [4]. They are not only environmentally acceptable but also inexpensive, readily available and renewable source of materials [4].

As a part of our ongoing research work regarding the application of natural products as corrosion inhibitor for aluminium and aluminium alloys [5-7], we report herein, the results of utility of Carica papaya seed extract (CPSE) for the corrosion control of aluminium at the pH of 2.6. This study has dual purposes, first to study the corrosion behavior of aluminium at lowest possible concentration of sulphuric acid medium and secondly to establish the effectiveness of the plant extract (CPSE) as corrosion inhibitor.
Carica papaya plant belongs to the family of Carricaceae and widely available in South India. Papaya seeds are reported to have antibacterial properties and have many more therapeutic uses [8]. References are available for using Carica papaya seed extract for corrosion control of steel in acid medium [9]. No reports are available till date, for the use of CPSE as corrosion inhibitor for aluminium in sulphuric acid medium by electrochemical techniques.

MATERIALS AND METHODS

Materials: The composition of aluminium is: Si: 0.467%, Fe: 0.163%, Mg: 0.530% and aluminium: Balance. Cylindrical test coupons of 10 mm diameter and approximately 20 mm height were machined from the rods of aluminium and metallographically mounted up to 10mm height using cold setting resin. The exposed flat surface of the mounted part was polished as per standard metallographic practice - belt grinding followed by polishing on emery papers (240, 400, 600 and 800grades) and finally disc polished using levigated alumina abrasive.
Medium: The stock solution of 2M sulphuric acid was prepared by using Analar grade sulphuric acid and double distilled water and standardized by volumetric method. From the standard solution, sulphuric acid solution of required strength was prepared as and when required.
Preparation and characterization of seeds of Carica papaya seed extract (CPSE): The healthy papaya seeds were washed properly with water and shade dried completely and air-dried at room temperature for 4 weeks. The dried seeds were pulverized into fine powder using a domestic mixer grinder. The aqueous extract of the same was prepared by literature method [10]. 40 g of the powdered Carica papaya seeds were boiled in 500 ml of distilled water for 30 minutes after which it was filtered using a piece of clean white cotton gauze. The filtrate was evaporated to complete dryness at 40ºC, producing a fine sweet smelling and chocolate color solid residue. The solid residue obtained was weighed and pooled together in an air and water-proof container kept in a refrigerator at 4ºC. FTIR of the solid residue was recorded using spectrophotometer (Shimadz model) in the frequency range of 4000 to 400cm^{-1} using KBr pellet. Aqueous solutions of required strength were prepared whenever required.
Electrochemical measurements: Electrochemical measurements were carried out using a potentiostat (CH 600D series US Model with CH instrument beta software). Both polarization studies and EIS measurements were carried out using conventional three-electrode Pyrex glass cell with platinum counter electrode and saturated calomel electrode (SCE) as reference electrode. The working electrode was made up of aluminium sample. All the values of potential are referred to the SCE. The polarization studies were done immediately after the EIS studies on the same electrode without any further surface treatment. Polished aluminium specimen with 0.95cm^2 surface area was exposed to 50mL of sulphuric acid (pH=2.6) at 30°C without and with 50, 100, 200, 300 and 400ppm inhibitors in the acid solution and allowed to establish a steady-state open circuit potential (OCP). The potentiodynamic current–potential curves were recorded by polarizing the specimen to -250 mV cathodically and +250 mV anodically with respect to the OCP At a scan rate of 0.5 mVs^{-1}. Various potentiodynamic parameters were determined. The corrosion rate in mmy^{-1} was calculated using equation (1).

$$\upsilon_{corr} \ \text{mm y}^{-1} = \frac{3270 \text{ x } M \text{ x i}_{corr}}{\rho \text{ x } Z} \quad (1)$$

Where 3270 is a constant that defines the unit of corrosion rate, i_{corr} = corrosion current density in A cm^{-2}, q = density of the corroding material, M = Atomic mass of the metal, and Z = Number of electrons transferred per metal atom [11].

The percentage inhibition efficiency was calculated from expression (2).

$$\eta(\%) = \frac{i_{corr} - i_{corr(inh)}}{i_{corr}} \times 100 \quad (2)$$

Where i_{corr} .and $i_{corr.(inh)}$ are the corrosion current densities in the absence and in the presence of inhibitor, respectively. The experiments were performed at 35 °C, 40 °C, 45 °C and 50 °C by keeping the cell in a calibrated thermostat. Corrosion potential (E_{corr}), corrosion current density. ($i_{corr.}$) were recorded and corrosion rate (CR) and % IE were determined.

The corrosion rates in all the above conditions were also obtained from electrochemical impedance measurement technique (EIS). It was carried out in a frequency range from 0.01 to 10000Hz using a small amplitude ac signal of 10mV at the open circuit potential. Impedance data were analyzed using Nyquist plots. Charge transfer resistance (R_{ct}) and double layer capacitance (C_{dl}) were recorded. The inhibition efficiency (n %) was calculated using equation (3)

$$n(\%) = \frac{RP(inh.) - RP}{RP(inh.)} \times 100 \quad (3)$$

where $Rp_{(inh.)}$ and R_p are the polarization resistances in the presence and absence of inhibitors.

Scanning electron microscopy: The surface morphology of aluminium surface, in absence and in the presence of the inhibitor was studied by immersing the material in sulphuric acid of pH 2.6 for 2 hrs. using JEOL JSM-6380L Analytical scanning electron microscope.

RESULTS AND DISCUSSION

Fourier transform infrared (FTIR) spectroscopy of CPSE: Figure 1 shows the FTIR spectrum of CPSE. –N=C=S Stretching frequency appears at 2300cm^{-1}.The Aromatic Stretching frequency appears at 3050cm^{-1}. The -C=C- Stretching frequency at 1612cm^{-1}.

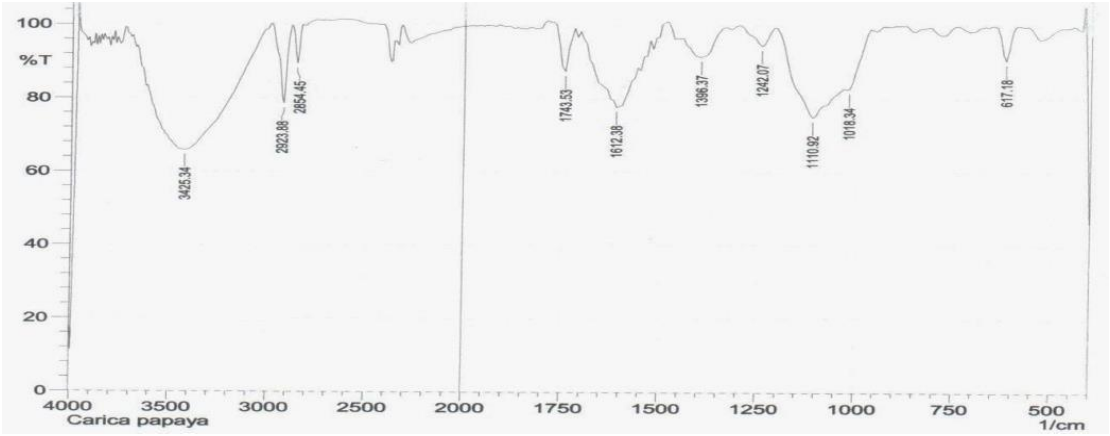

Fig. 1: IR spectra of CPSE

Potentiodynamic polarization curves: Figure 2 shows the Tafel polarization curves of aluminium in sulphuric acid of 2.6 pH at 30°C for different concentrations of inhibitor.

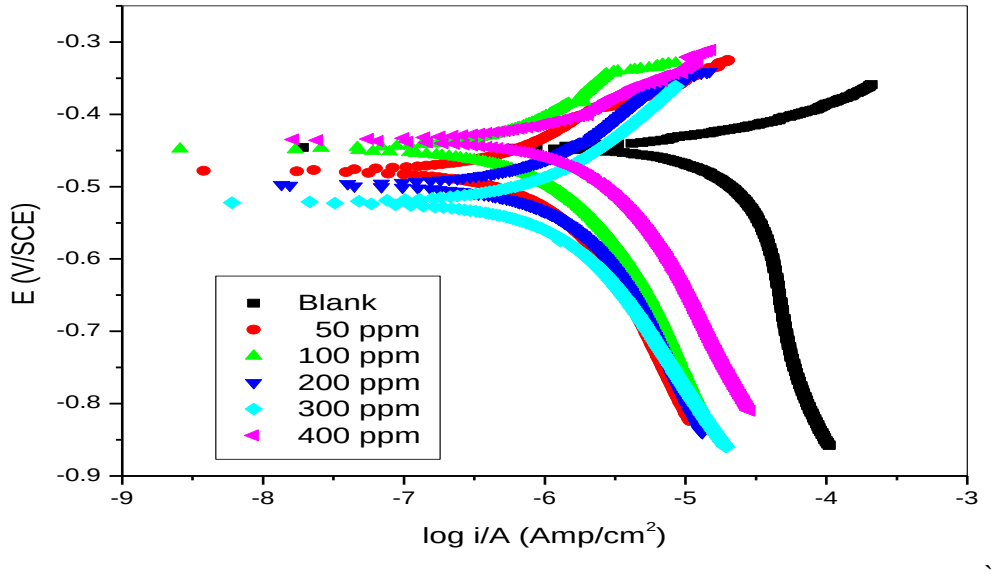

Fig. 2: Tafel plot for aluminium in H_2SO_4 of pH 2.6 at 30°C for different concentrations of CPSE

Valuable potentiodynamic polarization parameters like, corrosion current density ($i_{Corr.}$), corrosion potential ($E_{corr.}$), anodic and cathodic Tafel slopes (b_a and $-b_c$) were obtained from the Tafel plots. Corrosion rate and inhibition efficiency were calculated using the relations (1) and (2) respectively. The results are tabulated in Table 1. Table 1 reveals that with increase in the concentration of CPSE there was considerable decrease in the anodic and cathodic current densities. There was no remarkable change in the corrosion potential (E_{corr}). Inhibition efficiency increased with increase in inhibitor concentrations. The observed inhibition efficiency of CPSE was attributed to the adsorption of its components on the aluminium surface. The adsorbed molecules isolate the metal surface from the aggressive medium leading to decreasing the corrosion rate. At the concentration of 400ppm the inhibition efficiency of extract reached maximum of 96.71%.

Table 1: Results of Tafel polarization studies of aluminium in sulphuric acid of pH 2.6

Temp. (°C)	Conc.of inhibitor (ppm)	$i_{Corr.}$ ($\times 10^{-5}$ A/cm^{2})	C.R. (mmpy)	ba (mV/dec^{-1})	-bc (mV/dec^{-1})	$E_{corr.}$ (mV vs SCE)	Ƞ (%)
30	0	3.77	0.45	0.44	0.27	− 527	-----
	50	0.54	0.24	0.53	0.47	− 544	85.74
	100	0.28	0.04	0.61	0.43	− 540	92.45
	200	0.24	0.03	0.63	0.48	− 488	93.66
	300	0.22	0.02	0.65	0.49	− 520	94.29
	400	0.12	0.01	0.52	0.46	− 481	96.71
35	0	4.91	0.44	0.40	0.27	− 553	-----
	50	0.80	0.36	0.52	0.48	− 530	83.61
	100	0.43	0.08	0.62	0.44	− 519	91.22
	200	0.35	0.04	0.65	0.43	− 500	92.94
	300	0.32	0.03	0.65	0.46	− 482	93.52
	400	0.26	0.02	0.73	0.46	− 480	94.78
40	0	5.43	0.57	0.36	0.30	− 600	-----

	50	0.87	0.39	0.45	0.47	− 621	83.89
	100	0.52	0.11	0.56	0.53	− 603	90.43
	200	0.43	0.11	0.59	0.47	− 580	92.11
	300	0.36	0.11	0.60	0.42	− 583	93.40
	400	0.34	0.07	0.62	0.50	− 561	93.77
45	0	5.48	0.60	0.33	0.44	− 633	-----
	50	0.88	0.40	0.48	0.52	− 620	83.89
	100	0.63	0.37	0.53	0.48	− 630	88.50
	200	0.58	0.17	0.57	0.46	− 634	89.30
	300	0.44	0.16	0.61	0.44	− 635	92.00
	400	0.42	0.16	0.63	0.58	− 640	92.25
50	0	5.68	0.66	0.33	0.58	− 605	-----
	50	1.51	0.50	0.50	0.54	− 600	73.37
	100	0.71	0.19	0.51	0.52	− 623	87.50
	200	0.70	0.12	0.53	0.53	− 627	87.62
	300	0.69	0.11	0.61	0.50	− 630	87.87
	400	0.67	0.10	0.55	0.47	− 630	88.12

The parallel cathodic Tafel curves suggest that the hydrogen evolution is activation controlled, and the reduction mechanism is not affected by the presence of the inhibitors [12]. The values of $-b_c$ changed with increase in inhibitor concentration which indicates the influence of seeds of Carica papaya on the kinetics of hydrogen evolution. The shift in the anodic Tafel slope b_a may be due to the sulfate/ inhibitor molecules adsorbed on the aluminium surface.

Careful observation of E_{corr} values indicates that shift in the corrosion potential is less than 85mV at almost all measured temperatures. This is suggestive of the fact that corrosion inhibitor may act as mixed type [12]. According to Ferreira et al and Li et al.[13, 14], if the displacement in corrosion potential is more than ±85 mV with respect to corrosion potential of the blank, then the inhibitor can be considered as a cathodic or anodic type. It is evident from Table 1 that, even though average shift in corrosion potential is less than 85mV, change is more towards the positive or anodic side. It can be therefore inferred that, the inhibitor CPSE, acts as a mixed type of inhibitor with predominate inhibitive action at the anodic sites.

Electrochemical impedance spectroscopy (EIS) studies: In order to gain more information about the corrosion inhibition phenomenon, electrochemical impedance spectroscopy measurements were carried out for the aluminium in sulphuric acid medium of pH 2.6 in the presence and absence of aqueous extracts of seeds of Carica papaya at different temperatures. Figure 3 represent Nyquist plot of aluminium in the presence of various concentrations of aqueous extracts of seeds of Carica papaya in a solution containing sulphuric acid of pH 2.6 at 30°C. Similar results were obtained at other temperatures studied.

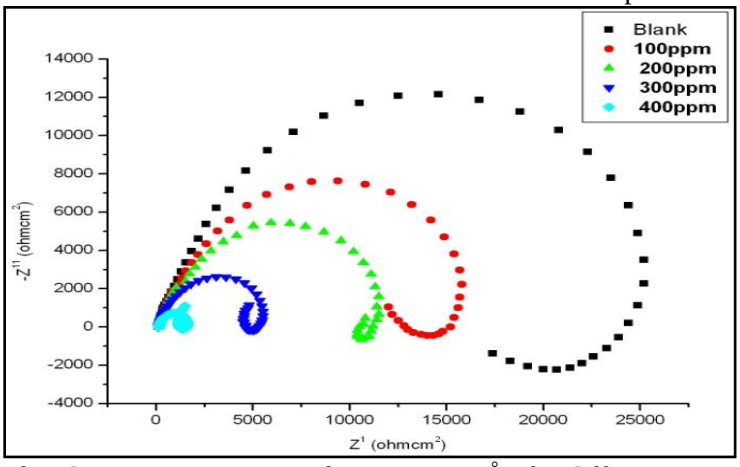

Fig. 3: Nyquist plot for aluminium in H_2SO_4 of pH 2.6 at 30 °C for different concentrations of CPSE

As can be seen from figure 3 the impedance diagrams show semicircles, indicating that the corrosion process is mainly charge transfer controlled. The presence of inhibitor increases the impedance but does not change other aspects of the behavior. These results support the results of polarization measurements that the inhibitor does not alter the mechanism of electrochemical reactions responsible for corrosion. It inhibits corrosion primarily through its adsorption on the metal surface [15]. The impedance plots are with a depressed capacitive loop at high-frequency range (HF) whose diameter increases with increase in inhibitor concentration, followed by an inductive loop at low-frequency (LF) region. Similar impedance plots have been reported in the literature for the corrosion of pure aluminum and aluminum alloys in various electrolytes [16–17].The impedance parameters derived from Nyquist plots and inhibition efficiency of seeds of Carica papaya in sulphuric acid of pH 2.6 at different temperatures are given in table 2.

Table 2: EIS data of aluminium in sulphuric acid of pH 2.6 in the presence of different concentrations of aqueous extracts of seeds of Carrica papaya

Temp. (^{0}C)	Conc. Of inhibitor (ppm)	C_{dl} ($\times10^{-10}$F/cm^2)	R_{ct} (ohmcm^2)	ɳ %
30	0	124.5	1599.8	----
	50	24.9	8070.1	80.2
	100	9.7	14604.8	89.0
	200	6.8	15363.7	89.6
	300	5.4	18264.7	91.2
	400	4.8	19262.2	91.6
35	0	215.1	1305.3	----
	50	48.6	5193.5	74.9
	100	22.5	9812.2	86.6
	200	18.4	11795.3	88.9
	300	12.0	12329.4	89.4
	400	9.6	14158.8	90.7
40	0	296.7	1143.7	----
	50	66.5	4964.9	76.9
	100	41.8	6585.9	82.0
	200	30.5	8143.0	85.9
	300	25.3	9812.2	88.3
	400	16.7	11517.4	90.0
45	0	436.4	1038.1	----
	50	140.4	4264.9	75.6
	100	96.3	5563.4	81.3
	200	86.7	6027.4	82.7
	300	42.3	6328.0	83.6
	400	38.0	6975.7	85.1
50	0	893.6	866.1	----
	50	230.1	3127.9	72.3
	100	101.1	4278.8	79.8
	200	71.0	4869.2	82.2
	300	48.2	5135.1	83.1
	400	31.9	5358.7	83.8

The high frequency capacitive loop could be assigned to the charge transfer of the corrosion process and to the formation of oxide layer [18]. The oxide film is considered to be a parallel circuit of a resistor due to the ionic conduction in the oxide film and a capacitor due to its dielectric properties. According to Brett [19], the capacitive loop is corresponding to the interfacial reactions, particularly, the reaction of aluminum oxidation at the metal/oxide/electrolyte interface. The process includes the formation of Al^+ ions at the metal/oxide interface, and their migration through the oxide/solution interface where they are oxidized to Al^{3+}. At the oxide/solution interface, OH^- or O^{2-} ions are also formed. The fact that all the three processes are represented by only one loop could be attributed either to the overlapping of the loops

of processes, or to the assumption that one process dominates and, therefore, excludes the other processes [20]. The other explanation offered to the high frequency capacitive loop is the oxide film itself. This was supported by a linear relationship between the inverse of the capacitance and the potential found by Bessone et al. [21] and Wit and Lenderink [22]. The origin of the inductive loop has often been attributed to surface or bulk relaxation of species in the oxide layer [23]. The LF inductive loop may be related to the relaxation process obtained by adsorption and incorporation of sulphate ions, oxide ion and charged intermediates on and into the oxide film. The measured values of polarization resistance increase with the increasing concentration of aqueous extracts of seeds of Carica papaya in the solution, indicating decrease in the corrosion rate for the aluminium with increase in inhibitor concentration. This is in accordance with the observations obtained from potentiodynamic measurements.

An equivalent circuit of nine elements depicted in figure 4a was used to simulate the measured impedance data of the aluminium. It is as shown in figure 4b.

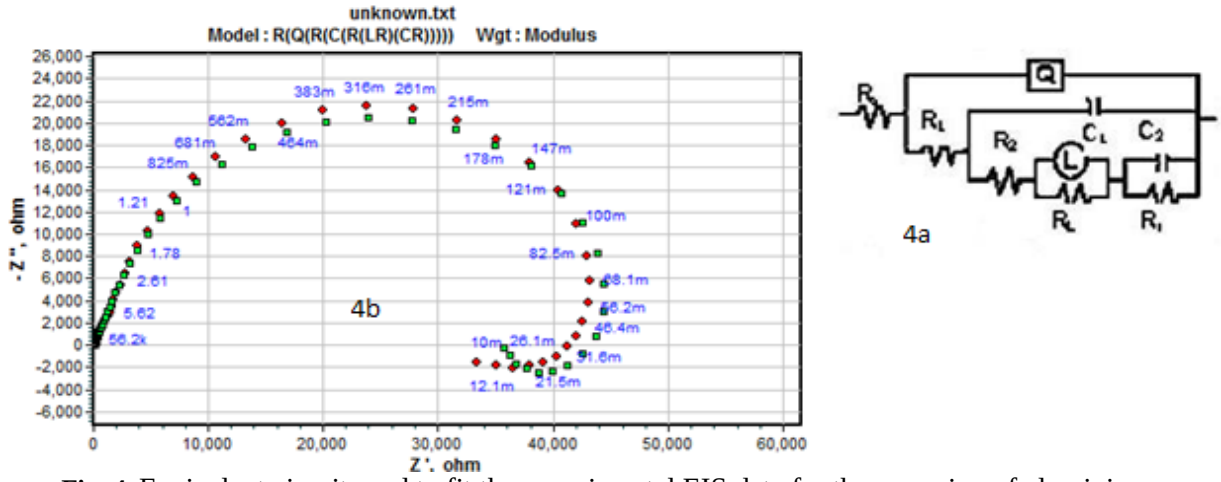

Fig. 4: Equivalent circuit used to fit the experimental EIS data for the corrosion of aluminium

In this equivalent circuit R_s is the solution resistance and R_t is the charge transfer resistance. R_L and L represents the inductive elements. CPE (Q) is constant phase element in parallel to the series capacitors C_1, C_2 and series resistors R_1, R_2, R_L and R_t. R_L is parallel with the inductor L.

The double layer capacitance C_{dl} can be calculated from equation (4)

$$C_{dl} = C_1 + C_2 \quad (4)$$

And the polarization resistance R_p is calculated using the equation (5)

$$R_p = R_L + Rt + R_1 + R_2 \quad (5)$$

Since R_p is inversely proportional to the corrosion current and it was used to calculate the percentage inhibition efficiency using the relation (3).

As seen from figure 3 that R_s (solution resistance) remains almost constant, with and without addition of aqueous extracts of seeds of Carica papaya for aluminium. It was also observed that the value of constant phase element Q, decreases, while the values of R_t increase with increasing concentration of inhibitor, indicating that the inhibition efficiency increases with the increase in concentration of aqueous extracts of seeds of Carica papaya. The double layer between the charged metal surface and the solution is considered as an electrical capacitor. The adsorption of inhibitor on the aluminum surface decreases its electrical capacity because they displace the water molecules and other ions originally adsorbed on the surface. The decrease in this capacity with increase in inhibitor concentrations may be attributed to the formation of a protective layer on the electrode surface. The thickness of this protective layer increases with increase in inhibitor concentration up to their critical concentration and then decreases. The obtained CPE (Q) values decrease noticeably with increase in the concentration of inhibitors.

Effect of temperature: It can be seen from Table 1 that % I.E. increased with concentration of the extracts but decreased with increase in temperature. This is attributed to the decrease in the protective nature of the inhibitive film formed on the metal surface (or desorption of the inhibitor molecules from the metal surface) at higher temperatures [24]. This suggests physical adsorption mechanism. Physical (electrostatic) adsorption takes place when inhibition efficiency decreases with increase in temperature (whereas chemical adsorption takes place when inhibition efficiency increases with increase in temperature). However, at higher concentration of inhibitor this decrease is small. The study of effect of temperature was used to calculate energy of activation (E_a) for the corrosion process in the presence and absence of inhibitor using Arrhenius law Equation (6) [25].

$$\ln (CR) = B - (\frac{Ea}{RT}) \quad (6)$$

where B is a constant which depends on the metal type and R is the universal gas constant, T is the absolute temperature. The Arrhenius plots for the aluminum are shown in figure 5. The plot of ln (CR) versus 1/T gives straight line whose slope = $-E_a/R$ gives activation energy for the corrosion process.

The entropy and enthalpy of activation values (ΔH_a& ΔS_a) for the dissolution of specimen were calculated from transition state Equation (7) [25].

$$CR = RT\frac{RT}{Nh}\exp(\frac{\Delta Sa}{R})\exp(-\frac{\Delta Ha}{RT}) \quad (7)$$

where h is Plank's constant and N is Avogadro's number.

A plot of ln (corrosion rate/T) versus 1/T gives straight line with slope = -ΔHa/R and intercept = ln(R/Nh) +ΔSa/R. The calculated values of E_a, ΔH_a and ΔS_a are given in table 3.

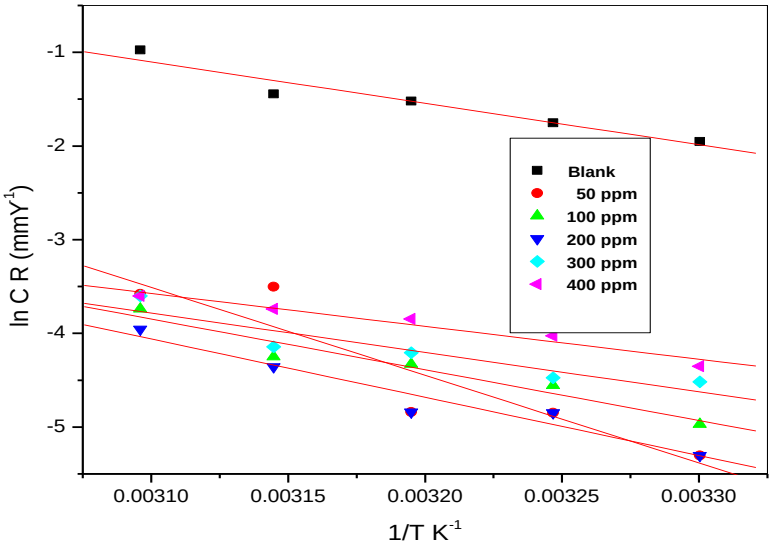

Fig. 5: Plot of ln (CR) Vs 1/T

Table 3: Activation parameters for the corrosion of aluminium

[CPSE] (ppm)	E_a (kJ mol^{-1})	R^2	ΔH_a (kJ mol^{-1})	ΔS_a (JK^{-1}mol^{-1})
0	29.20	0.99	27.82	− 246.04
50	36.70	0.97	31.31	− 205.91
100	34.97	0.99	32.37	− 217.86
200	51.70	0.96	34.09	− 218.41
300	45.02	0.98	42.42	− 249.03
400	77.87	0.97	49.10	− 267.97

The plot of ln (corrosion rate/T) versus 1/T for the aluminium in various concentrations of inhibitor in sulphuric acid of pH 2.6 is shown in figure 6.

The increase in activation energy (E_a) of inhibited solutions compared to the blank suggests that inhibitor is physically adsorbed on the corroding metal surface, while either unchanged or lower energy of activation in the presence of inhibitor suggest chemisorption [26]. As reported in Table 3, E_a values increased significantly after the addition of the inhibitor. Hence corrosion inhibition of seeds of Carica papaya is occurring through physical adsorption. The increase in the E_a values, with increasing inhibitor concentration indicates the increase in energy barrier for the corrosion reaction, with the increasing concentrations of the inhibitor. The adsorption of the inhibitor molecules on the surface of the aluminium blocks the charge transfer during corrosion reaction, thereby increasing the activation energy. In other words, the adsorption of the inhibitor on the electrode surface leads to the formation of a physical barrier that reduces the metal reactivity in the electrochemical reactions of corrosion [27].

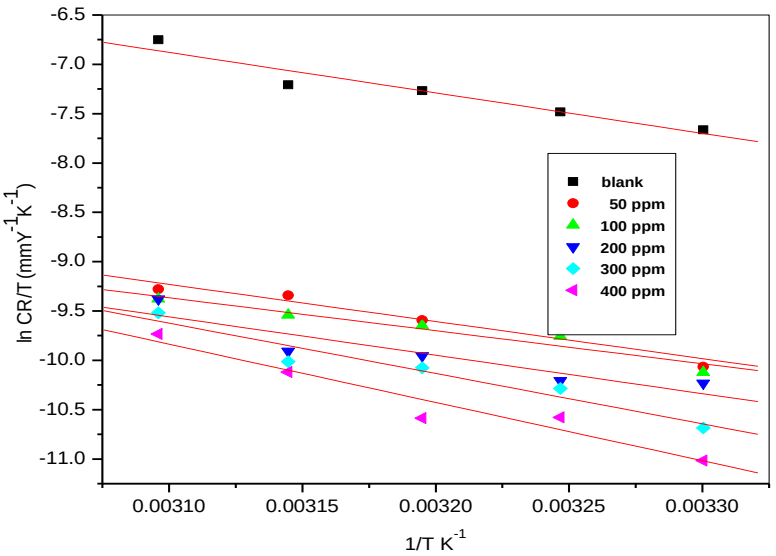

Fig. 6: Plot of ln (CR/T) Vs 1/T

The inhibition efficiency decreased with increase in temperature. It indicates desorption of inhibitor molecule with increase in temperature [28]. The values of ΔS_a are higher for inhibited solutions than those for the uninhibited solutions. This suggested that an increase in randomness occurred on going from reactants to the activated complex. This might be the results of the adsorption of organic compound present in the seeds of Carica papaya from the acidic solution which could be regarded as a quasi-substitution process between the organic compound in the aqueous phase and water molecules at electrode surface. In this situation, the adsorption of inhibitor is accompanied by desorption of water molecules from the surface. Thus the increase in entropy of activation was attributed to the increase in solvent entropy [29].

Adsorption Isotherm: Inhibitors are known to decrease metal dissolution via adsorption on the metal/corrodent interface to form a protective film which separates the metal surface from the corrosive medium. The adsorption route is usually regarded as a substitution process between the inhibitor in the aqueous solution [Inh (sol)] and water molecules adsorbed at the metal surface [$H_2O_{(ads)}$] as given below [30].

$$Inh_{(sol)} + nH_2O_{(ads)} \leftrightarrow Inh_{(ads)} + nH_2O_{(sol)} \quad (8)$$

where n represents the number of water molecules replaced by one molecule of adsorbed inhibitor. The adsorption bond strength is dependent on the composition of the metal, corrodent, inhibitor structure, concentration and orientation as well as temperature. Adsorption isotherms are usually employed to explain the mechanism of interaction between an inhibitor (adsorbate) and an adsorbent surface. This is usually achieved by fitting the degree of surface coverage data into various adsorption isotherms or models

and the correlation coefficients (highest) used to determine the best fit isotherm which can then be used to describe the inhibitor adsorption mechanism. In this work, the best fitted isotherm was the Langmuir adsorption model which relates the degree of surface coverage (θ) to the concentration of the extracts ($C_{inh.}$) according to equation (9).

$$\frac{\theta}{1-\theta} = \text{Kads.C} \quad (9)$$

where K_{ads} is the equilibrium constant of the inhibitor adsorption process and C is the inhibitor concentration, and θ is the degree of the surface coverage, which is calculated using Equation (10).

$$\theta = IE\%/100 \quad (10)$$

where IE% is percentage inhibition efficiency as calculated using Equation (3).

This model has also been used for other inhibitor systems [30-31]. The plot of C_{inh}/θ versus C_{inh} gives a straight line with intercept 1/K as shown in Figure 7.The values of standard free energy of adsorption are related to K by the relation (11).

$$\Delta G^0_{ads} = -RT\ln\frac{55.5\theta}{C(1-\theta)} \quad (11)$$

where the value 55.5 is the concentration of water in solution in M (mol L^{-1}), R is the universal gas constant and T is absolute temperature [32]. The thermodynamic data obtained from adsorption isotherm are tabulated in table 4. The correlation coefficient (R^2) was used to choose the isotherm that best fit the experimental data. The linear regression coefficients are close to unity, and the slopes of straight lines are nearly unity, suggesting that the adsorption of organic compounds present in the seeds of Carica papaya obeys Langmuir's adsorption isotherm, and there is negligible interaction between the adsorbed molecules [19]. The high values of K for the studied inhibitor indicate strong adsorption of inhibitor on the metal surface. The value of K increases with increase in inhibitor concentration also indicates the physical adsorption of the inhibitor on the metal surface. The negative values of ΔG^0_{ads} suggest the spontaneous adsorption of inhibitor on the surface of metal and the stability of the adsorbed layer on the aluminium. In general, the standard free energy values of -20 kJ mol^{-1} or less negative are associated with an electrostatic interaction between charged molecules and charged metal surface, resulting in physisorption, and those of -40 kJ mol^{-1} or more negative involve charge sharing or transfer from the inhibitor molecules to the metal surface to form a coordinate covalent bond, resulting in chemisorptions [30]. The ΔG^0ads values obtained for the studied inhibitor on the aluminium surface in sulphuric acid of pH 2.6 range from −16.69 to −17.74kJ mol^{-1}, indicating physical adsorption. The ΔG^0_{ads} values obtained for the studied inhibitor was found to decrease with increasing temperature supports that inhibitor is physisorbed on the surface of aluminium.

A plot of $\Delta G°_{ads}$ versus T was used to calculate the heat of adsorption $\Delta H°_{ads}$ and the standard adsorption entropy $\Delta S°_{ads}$ according to the thermodynamic Equation (12). The plot of $\Delta G°_{ads}$ versus T is given in figure 8.

$$\Delta G^0_{ads} = \Delta H^0\text{ads} - T\Delta S^0\text{ads} \quad (12)$$

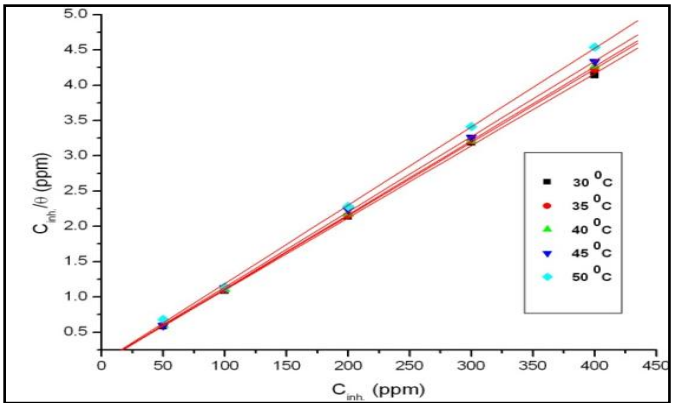

Fig. 7: Langmuir adsorption isotherms for the adsorption of CPSE on aluminium

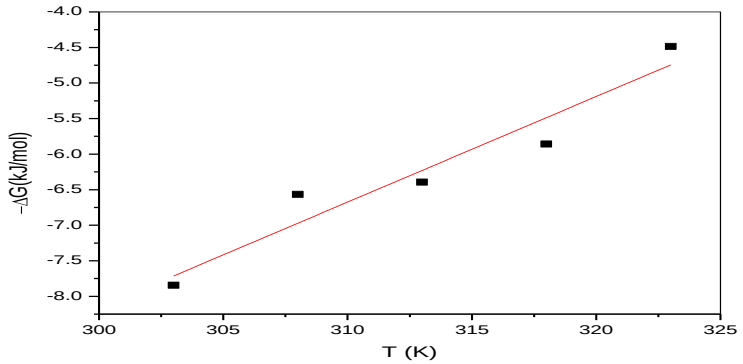

Fig. 8: Plot of free energy of adsorption versus T

The values of thermodynamic parameters for the adsorption of inhibitors can provide valuable information about the mechanism of inhibition. While an endothermic adsorption process (ΔH^0ads> 0) is attributed unequivocally to chemisorptions, an exothermic adsorption process (ΔH^0ads <0) may involve either physisorption or chemisorption or a mixture of both the processes. In an exothermic process, physisorption is distinguished from chemisorption by considering the absolute value of adsorption enthalpy. Typically, the enthalpy of a physisorption process is lower than 41.86kJ mol^{-1}, while that of a chemisorption process approaches 100kJ mol^{-1}[33]. In the present case, the calculated value of ΔH^0_{ads} is -0.11kJ mol^{-1}, which is a physisorption. The ΔS^0_{ads} value is negative, indicating that an ordering takes place when the inhibitor gets adsorbed on the metal surface.

Table 4: Adsorption parameters for the corrosion of aluminium

Temp. (^{0}C)	K	R^2	ΔG^0 (kJ mol^{-1})	ΔH^0 (kJ mol^{-1})	ΔS^0 ($JK^{-1}mol^{-1}$)
30	0.10	0.99	− 16.61		
35	0.06	0.99	− 17.06		52.70
40	0.05	0.99	− 17.54	− 0.11	-0.05
45	0.05	0.99	− 17.61		
50	0.04	0.99	− 17.70		

Scanning Electron Microscopy and Energy-dispersive X-ray spectroscopy (EDX) analysis: The SEM images were recorded to establish the interaction of acid medium with the metal surface using JEOL JSM-6380LA analytic scanning electron microscope. The surface morphology of the aluminium was examined by SEM immediately after the sample is subjected to corrosion in H_2SO_4 medium of pH 2.6 in the absence and in the presence of inhibitor. The SEM image of corroded aluminium in figure 9(a) shows degradation of sample in the absence of inhibitor. Figure 9(b) represents SEM image of aluminium after the corrosion tests in a medium of sulphuric acid containing aqueous extracts seeds of Carica papaya. The image clearly shows the adsorbed layer of inhibitor molecules on the metal surface thus protecting the metal from corrosion.

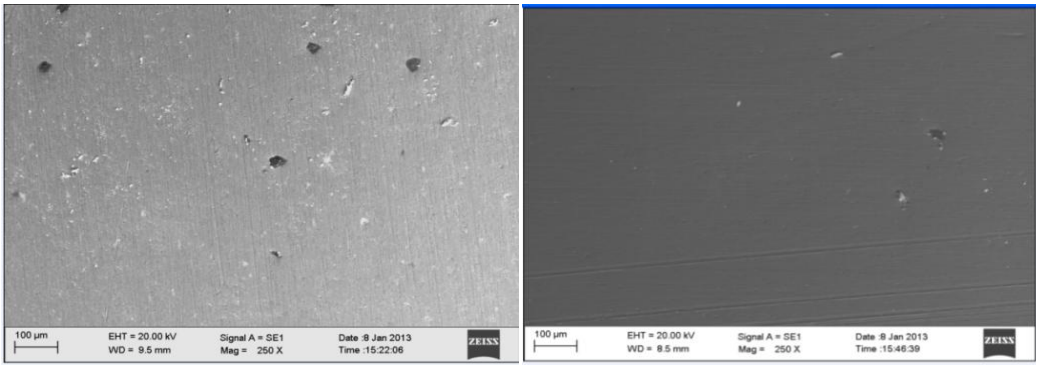

Figure 9(a): SEM image for Al metal in H_2SO_4 of pH 2.6 **9(b):** SEM image for Al metal in H_2SO_4 of pH 2.6+CPSE

Table 5 gives the EDX analysis result of aluminium in sulphuric acid of pH 2.6 in the absence and presence of CPSE inhibitor. Increase in the percentage content of nitrogen suggests the adsorption of inhibitor molecule on the surface of the metal, through the coordination bond.

Table 5: EDX analysis result of aluminium in H_2SO_4 in the presence and absence of CPSE

Medium	Composition (%)				
	Al	O	Si	S	N
Aluminium in sulphuric acid of pH 2.6	92.48	7.16	0.37	0.16	-
Aluminium in sulphuric acid of pH 2.6 in CPSE	79.02	7.16	0.38	0.06	0.28

Mechanism of Inhibition: CPSE is composed of numerous naturally organic heterocyclic compounds. Principal active constituent of CPSE is reported [10] to be benzylisothiocyanate the structure of same is given in figure 12.

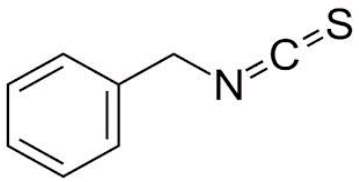

Fig. 10: Structure of Benzylisothiocyanate

Surface of aluminium is covered with thin layer of γ alumina which initially thickens on exposure to neutral aqueous solution with the formation of a layer of crystalline hydrated alumina. On exposure to acidic environment, the layer becomes thin due to corrosion. According to reported literature [34,35] corrosion of aluminium in acidic medium proceeds according to the following mechanism:

Anodic reaction:

$Al + H_2O \rightarrow AlOH_{(ads)} + H^+ + e^-$ (13)

$AlOH_{(ads)} + 5H_2O + H^+ \rightarrow Al^{3+} + 6H_2O + 2e^-$ (14)

$Al^{3+} + H_2O \rightarrow [AlOH]^{2+} + H^+$ (15)

$[AlOH]^{2+} + X^- \rightarrow [AlOHX]^+$ (16)

Cathodic reaction

$H^+ + e^- \rightarrow H(ads)$ (17)

$H(ads) + H(ads) \rightarrow H_2$ (18)

Benzyl isothiocyante contains nitrogen and sulphur as heteroatoms in its moiety. These hetero atoms are rich source of electrons. They can easily form coordinate bond with the positively charged metal species. They form a protective barrier on the anodic region of the metal, bringing down the anodic process under control. From the observed shift in the corrosion potential (E_{corr}), it has been found that the inhibitor may also act as mixed inhibitor. In the acidic environment of pH=2.6, the inhibitor molecule gets protonated. This protonated inhibitor molecule forms a protective barrier on the cathodic site, blocking the evolution of hydrogen gas. Thus CPSE acts as mixed inhibitor, by inhibiting both anodic and cathodic reactions.

APPLICATIONS

CPSE has very high inhibition efficiency of 96% at a low concentration of 400 ppm. It can be effectively used as inhibitor for the corrosion control of aluminium in sulphuric acid medium. Sulphuric acid is used as pickling agent in almost all process industries. CPSE emerged as a cost effective green inhibitor, which

is not only environmentally benign, but also renewable source. It may become a potential ecofriendly natural inhibitor, as it can overcome some of the limitations of synthetic chemical inhibitors.

CONCLUSIONS

Potentiodynamic polarization and electrochemical impedance methods were used to evaluate the ability of aqueous Extracts of seeds of Carica papaya to inhibit corrosion of aluminium in sulphuric acid at pH 2.6. The principle conclusions are

- The corrosion of aluminium in sulphuric acid at pH 2.6 is significantly reduced by the addition of CPSE
- The inhibition efficiency increased with increase in inhibitor concentration and decreased with increase in temperature.
- CPSE is found to behave like mixed type of inhibitor
- CPSE followed Langmuir's model and adsorption took place by physisorption.
- The inhibition efficiency obtained from potentiodynamic polarization, and EIS techniques are in good agreement

REFERENCES

[1] M.Abdulwahab, A. Kasim, O.S.I.Fayomi,F.A. Suke, A.P.I.Popoola, *J. of Materi. Environ. Sci.*, **2012** 3, 1177.
[2] L.A.Nnanna,I.U. Anozie, C.S.Akoma, I.M.Mejeha,K.B. Okeoma, K.I.Mejeh, *Am. J. of Mater. Sci.***2011,** 1,76.
[3] M.A.Chidiebere, C.E.Ogukwe, K.L.Oguzie, C.N.Eneh, E.E.Oguzie ,*J. Ind. Eng. Chem. Res.*,**2012** 51, 668.
[4] N.Kumpawat, A.Chaturvedi, R.K.Upadhyay *Res. J. of Chem. Sci.*, **2012** 2, 51.
[5] Deepa Prabhu, Rao Padmalatha, *J. of Mater. Environ. Sci.*, **2013**, 4, 5,732-743.
[6] D. Prabhu, P. Rao, *J. of Environ. Chem. Eng.* **2013**, 1(4) 676-683
[7] Deepa, P., Padmalatha, *Arabian J. of Chem*, **2013**. http://dx.doi.org/10.1016/j.arabjc.2013.07.059
[8] G.Aravind, DebjitBhowmik 1,S Duraivel,G. Harish, *J. of Medi. Pla. Stu.*, **2013**, **1**, 1,7-15.
[9] Fabrizio Zucchi, Ibrahim Hashi Omar, *J. of Surf. Tech.*, **1985**, 24**,**391-399.
[10] A.A.Adeneye, J.A.Olagunju, A.A.F.Banjo,S.F.Abdul, O.A.Sanusi, O.O.Sanni, B.A.Osarodion, O.E.Shonoiki, *Int. J. of App. Res Nat. prod.*, **2009,** 2, 19-32.
[11] MG.Fontana, Corrosion engineering,. McGraw-Hill, Singapore, **1987**,106, 3rd edn.
[12] Li WH, He Q, Pei CL, Hou BR *J. of Electrochim.Acta,* **2007**, 52, 6386.
[13] E.S.Ferreira ES, Giancomelli C, Giacomelli FC, A.Spinelli *J. of Mater Chem.Phys.,* **2004,** 83,129.
[14] Li WH, He Q, Pei CL, Hou BR *J. of Appl. Electrochem.*,**2008**,38, 289.
[15] M.A.Amin, S.S.Abd El-Rehim, E.E.F. El-Sherbini, R.S.J. Bayyomi, *J. of Electrochim.Acta,* **2007** 52, 3588.
[16] C.M.A.Brett, *J. of Appl. Electrochem.*, **1990**, 20,1000.
[17] F.Mansfeld, S.Lin, K.Kim, H. Shih, *J. of Corros. Sci.*, **1987,** 27, 997.
[18] F.Mansfeld,S.Lin, S.Kim, H.Shih,*J. of Mater. Corros.*, **1988**, 39, 487.
[19] C.M.A.Brett, *J. of Corros. Sci.*, **1992,** 33, 203.
[20] J.H.Wit, H.J.W.Lenderink, *J. of Electrochim. Acta,* **1996**, 41, 1111.
[21] J.B.Bessone, D.R.Salinas, C.Mayer, M.Ebert, W.J. Lorenz, *J. of Electrochim. Acta***, 1992,** 37, 2283.
[22] S.E.Frers; M.M.Stefenel, C.Mayer, T.Chierchie, *J. of Appl. Electrochem.*, **1990**, *20*(6), 996–999.
[23] Schorr M, Yahalom, *J. of Corros.Sci.*, **1972**, 12, 867.
[24] M.Bouklah,B. Hammouti,A. Aounti, T.Benhadda, *J. of Prog.Org. Coat.*, **2004,** 49, 227.

[25] F.B.Mansfeld, Corrosion mechanisms, Marcel Dekkar, New York, **1987,** 165-209.
[26] M.I.Awad, *J. of Appl. Electrochem.*, **2006**, 36, 10, 1163-1168.
[27] M.Sahin, S.Bilgic, H.Yilmaz, *J. of Appl. Surf. Sci.***2002,** 195, 1, 1-314.
[28] B.Ateya, B.E.El-Anadouli, F.M.El-Nizamy, *J. of Corros. Sci.* **1984,** 24,509.
[29] F. Mansfeld, Corrosion, **1973**, 29,1st edition.
[30] E.E.Oguzie, V.O.Njoku, C.K.Enenebeaku, C.O.Akalezi, C.Obi, *J. of Corros. Sci* , **2008**, 50,3481.
[31] T.Sanaa Arab, *J. of Mater Res Bull*, **2008**, 43, 516.
[32] O.Olivares, N.V.Likhanova, B.Gomez, J.Navarrete, M.E.Llanos-Serrano, E.Arce, J.M.Hallen, *J. of Appl. Surf. Sci.*, **2006**, 252, 2894.
[33] B.Ateya, B.E.El-Anadouli, F.M.El-Nizamy, *J. of Corros. Sci.*, **1984,** 24, 509.
[34] Md. Nazrul Islam Bhuiyan, Jaripa Begum, Mahbuba Sultana, Bangladesh, *J. of Pharmacol.*, **2009,** 4, 150.
[35] O.K.Abiola, A.O.C.Aliyu, A.A.Phillips, A.O.Ogunsipe, *J. Mater. Environ. Sci.*, **2013,** 4, 370.